Environmental Science and Pollution Research
https://doi.org/10.1007/s11356-019-06222-7

RECENT ADVANCES AND NOVEL CONCEPTS IN ENVIRONMENTAL TECHNOLOGIES

Forcasting of an ANN model for predicting behaviour of diesel engine energised by a combination of two low viscous biofuels

Krishnamoorthy Ramalingam[1] · Annamalai Kandasamy[2] · Dhinesh Balasubramanian[3] · Moulik Palani[4] · Thiyagarajan Subramanian[5] · Edwin Geo Varuvel[5] · Karthikeyan Viswanathan[6]

Received: 20 March 2019 / Accepted: 16 August 2019

Abstract

This study is focused on artificial neural network (ANN) modelling of non-modified diesel engine keyed up by the combination of two low viscous biofuels to forecast the parameters of emission and performance. The diesel engine is energised with five different test fuels of the combination of citronella and *Cymbopogon flexuous* biofuel (C50CF50) with diesel at precise blends of B20, B30, B40, B50 and B100 in which these numbers represent the contents of combination of biofuel and the investigation is carried out from zero to full load condition. The experimental result was found that the B20 blend had improved BTE at all load states compared with the remaining biofuel blends. At 100% load state, BTE (31.5%) and fuel consumption (13.01 g/kW-h) for the B20 blend was closer to diesel. However, the B50 blend had minimal HC (0.04 to 0.157 g/kW-h), CO (0.89 to 2.025 g/kW-h) and smoke (7.8 to 60.09%) emission than other test fuels at low and high load states. The CO_2 emission was the penalty for complete combustion. The NO_x emission was higher for all the biodiesel blends than diesel by 6.12%, 8%, 11.53%, 14.81% and 3.15% for B20, B30, B40, B50 and B100 respectively at 100% load condition. The reference parameters are identified as blend concentration percentage and brake power values. The trained ANN models exhibit a magnificent value of 97% coefficient of determination and the high R values ranging between 0.9076 and 0.9965 and the low MAPE values ranging between 0.98 and 4.26%. The analytical results also provide supportive evidence for the B20 blend which in turn concludes B20 as an effective alternative fuel for diesel.

Keywords Citronella oil · Artificial neural network · Bio-fuel · Diesel engine · Emission · Simulation

Introduction

Globally, fossil energy plays a decisive character in each country's economy. It is proved that the availability of fossil fuel resource is only in gulf countries across the world which is the main reason for the monopoly in the fossil fuel trade. Mostly, all the vehicles including agriculture, transportation, industry and military depend on fossil fuels; therefore, the demand and cost of fossil fuels gradually increase (Mahmudul et al. 2017; Suresh et al. 2018; Manigandan et al. 2019a, b, c).

In addition, the rapid diminution of global oil reserves and growing atmospheric pollution threats such as global warming, which is alarmed to create awareness in searching for a renewable and environment-friendly fuel (Tamilselvan et al. 2017). So, renewable and biodegradable-based vegetable fuel is a better substitute for hydrocarbon fuels (Verma and Sharma 2016). In previous decades, diverse investigators have evaluated edible and non-edible vegetable oil in a

Responsible editor: Philippe Garrigues

✉ Thiyagarajan Subramanian
prashanth.86.1@gmail.com

1 Department of Mechanical Engineering, CK college of Engineering and Technology, Jayaram Nagar, Chellangkuppam, Cuddalore 607003, India

2 Department of Automobile Engineering, Madras Institute of Technology (MIT) Campus, Anna University, Chromepet, Chennai, Tamil Nadu 600044, India

3 Department of Mechanical Engineering, Mepco Schlenk Engineering College, Mepco Nagar, Mepco Engineering College Post, Sivakasi, Virudhunagar, Tamil Nadu 626005, India

4 Department of Industrial Engineering, Texas A & M University, 400 Bizzell St, College Station, TX 77843, USA

5 Green Vehicle Technology Research Centre, Department of Automobile Engineering, SRM Institute of Science and Technology, Kattankulathur, India

6 Department of Mechanical Engineering, Sri Krishna College of Engineering and Technology, Coimbatore 641 008, India

Published online: 05 September 2019

compression ignition engine successfully (Sakthivel et al. 2018). However, using raw oil in engines has some negative concern such as higher viscosity and lower heating value (Noor et al. 2018). Among them, high viscosity is the most significant factor affecting raw vegetable oil when used in a diesel engine. Hence, the transesterification process has evolved to shrink the viscosity (Szabados et al. 2018). But the transesterification process also has some negative concerns such us lower yield, minimal heating value and stability issues (Petranović et al. 2017).

Low viscous oil has been directly introduced to the CI engine without any secondary fuel quality improvement process like Transesterification process (Huang et al. 2016). Apparently, low viscous oil is directly synthesised from plant parts that have exclusive properties which are similar to natural diesel (Vallinayagam et al. 2014a). These kinds of low viscous oils yield many benefits that can be used in a diesel engine as a result of better atomization and greater evaporation caused by better viscous, lubricant property and presence of oxygen content. Besides that, the calorific value of all the low viscous oils is at most equivalent or comparable to diesel (Vallinayagam et al. 2014b; Ashok et al. 2018b; Rahman et al. 2019). In recent days many of the researchers had more interest in exploitation of low viscous fuels that are synthesised from *Cymbopogon flexuous*, lemongrass, eucalyptus, lemon peel, pine and camphor which can also be an influential alternative to diesel in a unmodified engine (Ashok et al. 2018a; Kumar et al. 2018). Furthermore, low viscous fuel researchers have to keen out on some advantages to say are superior atomization, greater air/fuel mixing property and improved engine performance. Evidently, these oils had superior combustion property owing to their better flash point and boiling point. Conversely, less viscous fuel had some negative obstacles such as improper lubrication property and high autoignition temperature (Purushothaman and Nagarajan 2009b; Anand et al. 2010). Current-day researchers also focus on synthesising the low viscous oil from the grass of various plants to replace the diesel usage in the CI engine (Purushothaman and Nagarajan 2009a). The steam distillation concept was employed to extract these grass-based renewable low viscous oils to be used in a diesel engine successfully (Kasiraman et al. 2012, 2016).

They tested their unmodified diesel engine powered with various blends of low viscous *Cymbopogon flexuous* grass oil with diesel and they revealed that 20% blend of *Cymbopogon flexuous* oil claimed a 6% drop in thermal efficiency and a 9% increment in fuel economy at the full load state when correlated with diesel. They also point out that 20% blend of *Cymbopogon flexuous* oil had minimal CP, ID and HRR. Interestingly EGT was higher owing to a better diffusion combustion phase than diesel, and also, they state that except CO_2 and NO_x, all the tailpipe emissions were lower than diesel for the reason of O_2 availability (Dhinesh et al. 2016b). Experimenting the PCCI engine fuelled with renewable lemongrass fuel, they noticed that HRR, ID and CP were shorter for lemongrass oil when correlated with diesel. They also report that lemongrass oil does not claim better engine efficiency(Alagumalai 2015). An attempt was made to increase the thermal efficiency of lemongrass oil by advancing the injection timing with higher fuel injection pressure which resulted in improved combustion and better thermal efficiency correlated with standard injection pressure and timing (Sathiyamoorthi and Sankaranarayanan 2016).

They derived lemon peel oil from waste lemon peel through the distillation process. The obtained thermochemical property of lemon peel oil is comparable to diesel. It was informed that the neat lemon peel oil exhibits a 12% increase in thermal efficiency and a 9% drop in fuel economy at the top load state. They also state that a considerable reduction has been noticed in CO, HC and smoke emission. However, the longer ignition lag of lemon peel oil inceases the CP and HRR. Consequently, LPO raised NO_x emission by 55% at the top load state (Ashok et al. 2017). They proved that low viscous pine oil demonstrates a better exhaust emission result than diesel fuel except for oxide of nitrogen on account of superior atomization, greater air/fuel mixing property and O_2 content (Vallinayagam et al. 2013).

Currently, there is a huge curiosity in mixing two or more biodiesels/biofuels obtained from different feedstocks with the intention of exploiting more benefits and many biofuel investigators supported this attempt and used these types of fuels in diesel engines effectively (Dubey and Gupta 2017, 2018). From combined fuel operation, they noticed a great improvement in physicochemical properties than single fuel operation. In addition, the combined biodiesel/biofuel achieve the ASTM standards (Dharma et al. 2017). The combined *Pongamia pinnata*-mustard biodiesel also had excellent engine effectiveness compared with any individual biodiesel/biofuel, by which engine economy was in the acceptable range at the maximum load state. Besides, a huge decline in CO, UBHC and smoke equated with other individual biodiesels/biofuels (Srithar 2017). They tested blended eucalyptus and paradise methyl ester oil in a CI engine. Interestingly, they noticed that BTE was 2.5% higher than diesel at 100% load state, and also, they reported that tailpipe emission of smoke, CO and HC are effectively reduced by 49%, 37% and 35% respectively (Devan and Mahalakshmi 2009).

They formulated a new innovation to mix the low viscous fuel with methyl ester fuel to be used in a CI engine. Their investigation indicates that the B25 and B50 blend had improved the BTE and BSEC at all load states. However, the B50 fuel significantly reduced in efficiency. They also indicate that there is a considerable reduction in CO, HC and smoke for the B50 blend at the top load state (Vallinayagam et al. 2014c). It is critical to ascertain the engine deeds

Table 1 Thermophysicochemical properties of citronella oil and *Cymbopogon flexuous* oil

Properties	Units	ASTM standards	Diesel	Citronella	*Cymbopogon flexuous*
Heating value	MJ/kg	ASTM D5865	44.52	37.19	37.01
Kinematic viscosity	Cst	ASTM D445	2.83	3.8	4.6
Density	kg/m3	ASTM D4052	820	897	899
Flash point	°C	ASTM D92	76	69	55
Boiling point	°C	ASTM D86	330	221	224
Cetane no.	–	ASTM D613	47	52	52

energised with biofuel-diesel blends that one may acquire broad records on the multifaceted effective environment. Nevertheless, experimental engine tests are very expensive on behalf of fuel cost, measurement charge, time and human effort. Hence, modelling skills are viable to appraise the engine characteristics (Çay et al. 2013; Kshirsagar and Anand 2017). Nevertheless, creating a precise model to forecast engine deeds is a discouraging job because numerous changes are considered in creating a model. Hence, the ANN has shown a possible solution because these methods enable the analysis of the physical phenomena of a complex system without the need of complex mathematical representation (Canakci et al. 2009; Sarıtas et al. 2010).

Among the various optimisation tools, ANN absorbs more attention owing to its robust operation and being less expensive in terms of time and cost (Ghobadian et al. 2009). In the last decade, numerous IC engine researchers employed the ANN to foretell its behaviour. The modelled ANN can foresee the performance components which are BTE, torque, BP, and fuel expenditure and emission components are HC, CO, NO_x and smoke. They observed a high-quality correlation between investigational and ANN forecast within 9% of MRE (Tosun et al. 2016).The researchers developed the ANN model to predict the engine deeds such as BTE, BSFC, EGT, NO_x, UBHC and smoke from that the overall mean relative errors were achieved less than 8% for methyl esters of rice bran fuelled in a CI engine. The result proved that ANN is very much suitable for forecasting the engine performance deeds (Rao et al. 2017). They investigated the diesel engine operation by the proposed ANN model to foresee the engine output deeds, namely BTE, BSFC, CO_2, NO_x and PM. They state that R and MAPE values are ranging from 0.987 to 0.999 and 1.1 to 4.5% respectively (Roy et al. 2014). Even though numerous investigators have been recognised regarding the analysis of the conventional CI engine with ANN. However, there is an insufficiency of lessons on the growth of ANN to forecast the engine deeds using two biofuels with diesel mixtures. The novelty of the research is escalated with the combination of dual low viscous biofuels.

Both low viscous citronella and *Cymbopogon flexuous* oils are extracted from their grass through the steam distillation process. These grasses are largely available in many places around India. The novelty of this experimentation prevails on the combination of two low viscous fuels that is to point out the blends made with citronella and *Cymbopogon flexuous* biofuel along with diesel at various amounts B20, B30, B40, B50 and B100 (B20 = 10% citronella oil + 10% *Cymbopogon flexuous* + 80% diesel), (B30 = 15% citronella oil + 15% *Cymbopogon flexuous* + 70% diesel), (B40 = 20% citronella oil + 20% Cymbopogon flexuous + 60% diesel), (B50 = 25% citronella oil +25% *Cymbopogon flexuous* + 50% diesel) and (B100 = 50% citronella oil + 50% *Cymbopogon flexuous*) used for testing in a conventional experimental engine and it is also escalated with the optimisation of the predictive data models using ANN, to predict the engine deeds.

Materials and methodologies

Description of low viscous oil

The citronella plant is a category the grass family with thin and long leaves. This herb is under the category of perennial and it grows up to 2-3 m in height. The width of leaves ranges around 10 mm to 20 mm and length is 1 to 2 m. It is mainly found in India, Srilanka, also found to a small extent in Taiwan, China and Africa (Guedes et al. 2018). The citronella grass is considered a hardy grass, which needs little care to grow. It can easily grow on any soil. It is sometimes planted on contour soils to prevent erosion. Habitually the herb is ready for harvesting after planting of 6 to 8 months. Consequent harvesting can be completed at an interval of 90 to 120 days. Period of harvesting has an undesirable effect on the quality of the extracted oil. It is a cost-effective herb as it brings into being a very imperative natural essential oil called citronella oil. The chief elements of this necessary oil were citronellol and geranial (Joy Prabu and Johnson 2015). It is broadly used in cosmetics industries all over the globe.

Cymbopogon flexuous also falls under the category of grass family with thin and long leaves, this grass belongs to the perennial aromatic type. It is fast growing type grass; grows up to height of 2.5 to 3meters. It was originally found in south India, middle Sri Lanka and later on found in China, Madagascar and Taiwan. It can be mature easily on variety

Table 2 Thermophysicochemical properties of C50CF50 biofuel and its blend

Properties	Units	ASTM standards	B20	B30	B40	B50	B100
Heating value	MJ/kg	ASTM D5865	43.6	42.3	41.2	39.8	37.15
Kinematic viscosity	Cst	ASTM D445	3.5	3.7	3.85	3.99	4.3
Density	kg/m3	ASTM D4052	840	853	861	879	898
Flash point	°C	ASTM D92	71	70	69	68	65
Boiling point	°C	ASTM D86	295	271	261	250	223
Cetane no.	–	ASTM D613	48	49	50	51	52

of soils, classically about unbiased pH level (Amine et al. 2018). The plant grows fine in warm and humid circumstances, at least necessitate 1500–2500 mm yearly rainfall. The *Cymbopogon flexuous* oil is a kind of natural essential oil with dark yellow colour and lemony flavour, the chief elements of this necessary oil were citral and geranyl acetate which is broadly used in cosmetics industries (Naser et al. 2018).

Preparation of low viscous oil

Both oils (citronella oil and *Cymbopogon flexuous* oil) were extracted by SDP (steam distillation process) because of economic and emission feasibility. The primary step in the extraction process was drying. Drying is a necessary action for lowering the water content and to increase the oil yield. SDP is a common method for withdrawing citronella and *Cymbopogon flexuous* oil. Most commonly, traditional type C distillation setup was employed to harvest the citronella and *Cymbopogon flexuous* oil. In distillation set-up, the shortened pieces are located in the top part of distillation chamber. Water is crammed in the bottom part and the assembly room is heated. The water is converted into steam by heat through the distillation chamber walls. This steam ultimately heats the shortened grass in the cap of the chamber. Oil in the grass is conceded away by steam. The haze consisting of oil and steam comes out from the distillation chamber and are engaged to the condenser. The condenser exemplifies the steam and oil and they are brought together in a container in which the oil is at top and water settles down in bottom owing to density discrepancy. The extracted oil is consists of impurities and frenzied to remove water substance to obtain pure oil. At last, the solid dust elements are isolated by 40 mm filter paper.

Property analysis of low viscous oil

Both the extracted citronella and *Cymbopogon flexuous* oil properties were satisfied with ASTM and EN standards. Quite a lot of tests were executed to establish the thermochemical properties of the extracted citronella and *Cymbopogon flexuous* oil for instance density, viscosity, CV, FP and CN are publicised in the Table 1.

FT-IR and GC-MS analysis

FT-IR was identified as a superior tool for identifying the characterization of biodiesel or biofuel; this is because of exactitude, simplicity and reproducibility (Dhinesh et al. 2016a). Made known by FT-IR of extracted oil, it is educated that numerous types of functional groups are in the extracted oil. In the scrupulous range of wavelength, the chemical bond of extracted oil was immersed in infrared radiation for the extent of the interface of infrared light from end to end of the extracted oil. Nicolet 550s series FTIR spectroscopy has

Table 3 Engine specification

Make	Kirloskar TV-1
Type	4-stroke, single-cylinder direct injection diesel engine
Cooling type	Water cooled
Bore	86.6 mm
Stroke	112 mm
Compression ratio	17.6:1
Rated power	5.2 kW
Rated speed	1500 rpm
Injection timing	23° before TDC
Nozzle	0.3 mm and 3 nozzles
Piston bowl type	Hemispherical

Table 4 Specification of emission Instruments

S. no.	Instrument	Type	Manufacturer	Measuring range
1	Smoke meter	AVL smoke meter	AVL India Pvt. Ltd.	0 to 100 HSU
2	Five gas analyzer	Krypton 290 five gas analyzer	SMS Auto line equipment's private limited	CO (0 to 10%) CO_2 (0 to 20%) HC (0 to10000 ppm) O_2 (0 to 25%) NO_x (0 to5000 ppm)

been employed to document the FTIR spectra of the known oil sample with the fascinating band array of 400–4000 cm^{-1}.

The GC-MS was employed for chemical investigations of both extracted citronella and *Cymbopogon flexuous* oil to discover the diverse chemical constitutes. The inspection was agreed with the assistance of the JEOL GC series system. At first, the initial temperature of the instrument was reset by about 50 °C for 2 min subsequently raised by 20 °C to reach 250 °C and 99.9 % pure helium carrier gas was utilised in the system with 1 ml/min flow rate. After all, GC-MS chamber temperature was 250 °C and the system is tied to a photomultiplier tube based on that; the chemical composition of extracted oil was acknowledged.

Test fuel preparation

The test fuel is prepared using a two-way flask at 25 °C and the speed of the stirrer is set to 1500 rpm for 15 min, the homogeneous mixture is obtained by two low viscous fuels extracted from citronella and *Cymbopogon flexuous*. Equal parts of both low viscous fuels are blended with diesel in five various proportions. The various proportionate fuels were tested for their physical and chemical properties in ETA lab Chennai using ASTM and EN standards. The properties are tabulated in Table 2.

Table 5 Uncertainty of different measuring parameters

Sl. no.	Measured parameters	Parentage uncertainty (%)
1.	Brake thermal efficiency	0.5
2.	Brake specific energy consumption	0.7
3.	Pressure	0.1
4.	Brake Power	0.3
5.	Fuel flow rate	0.5
6.	Air flow rate	0.6
7.	Carbon monoxide	0.14
8.	Carbon dioxide	0.14
9.	Hydro carbon	0.4
10.	Smoke	0.7
11.	Oxides of nitrogen	0.7

Experimental design and engine preparation

A mono cylinder agricultural and industrial application-based Kirloskar CI engine which is coupled with water-cooled Benz eddy current dynamo was used for this exploration. The engine is operated with different load conditions using a dynamometer; the engine generates 5.2 kW power with an IP of 200 bar and IT 23° before TDC and the elaborated technical data of the test engine is scheduled in Table 3. The test engine is engaged with DAS unit which calculates and documents the deeds (i.e. BTE, BSEC and BP). Furthermore, a smoke meter and a Krypton 290 gas tailpipe emission analyser were used to calculate and document the exhaust deeds that is to say CO, HC, NO_x and smoke. The emission instrument's technical data are scheduled in the Table 4.

Before starting the experiment, engine coolant flow and lubricant oil level were safeguarded to eliminate the overheating of the engine. Initially, the test was done with diesel at different load conditions 0%, 20%, 40%, 60%, 80% and 100% consequently. After obtaining baseline readings, the diesel fuel was drained. The test engine was fuelled with different blend fuels such as B20, B30, B40, B50 and B100 to evaluate engine performance and emission deeds. Forgetting accurateness of the outcome, each experiment was conducted up to five times. All the readings are noted down and it was presented and analysed as graphs.

Uncertainty evaluations

Logical and accidental errors often happen in the experimentation while reading, arranging the instrument and performing test. The instrument and equipment may not be of the same make and it is mandatory. The estimation of the uncertainties is important to approximate the results obtained from the instruments used. The present work is precise with back propagation uncertainty analysis to rectify the errors in the experimentation and has been calculated and tabulated in Table 5 by using the formula

Table 6 Prediction accuracy value for BTE, BSEC, CO, CO2, HC, NO_x and smoke using different training algorithms

Learning algorithm	Network structure	Prediction accuracy		Prediction accuracy		Prediction accuracy		Prediction accuracy		Prediction accuracy		Prediction accuracy		Prediction accuracy	
		BTE		BSEC		CO		CO_2		HC		NO_x		Smoke	
		Training set	Testing set	Training set	Testing set	Training set	Testing set	Training set	Testing set	Training set	Testing set	Training set	Testing set	Training set	Testing set
SCG	4-5-1	99.42	97.34	98.12	96.78	95.69	92.99	98.69	93.69	96.86	94.89	98.26	95.78	91.99	94.76
SCG	4-6-1	96.52	94.23	99.23	95.86	95.78	93.06	95.23	92.45	95.23	95.67	95.48	94.76	92.85	93.88
SCG	4-7-1	98.23	96.31	97.36	94.78	95.46	91.29	96.79	89.96	94.78	93.85	89.56	93.28	93.48	92.79
SCG	4-8-1	97.65	95.76	96.59	94.62	94.89	90.26	97.23	88.42	93.86	92.89	88.79	91.29	94.82	91.99
SCG	4-9-1	95.46	97.25	99.29	94.78	97.88	94.65	95.69	89.69	95.99	96.88	93.68	93.68	93.48	90.82
SCG	4-10-1	98.74	96.88	98.67	93.78	96.28	93.08	94.44	90.36	97.89	95.99	94.59	92.79	96.85	91.79
SCG	4-11-1	99.22	98.40	99.36	97.99	95.78	93.62	93.69	91.36	95.62	94.89	96.89	93.18	95.37	93.89
LM	4-5-1	98.74	91.34	98.16	96.99	91.69	91.28	99.01	92.63	94.78	93.69	92.89	94.56	94.99	94.79
LM	4-6-1	98.23	94.56	99.09	97.12	94.78	92.99	98.62	93.96	96.78	94.99	97.89	96.01	95.68	93.49
LM	4-7-1	97.26	95.76	99.76	97.09	92.69	93.67	97.25	94.99	93.79	95.62	95.28	95.78	96.31	92.88
LM	4-8-1	99.03	96.45	96.65	97.86	99.01	91.99	95.23	92.78	96.88	93.89	96.18	94.99	95.08	91.99
LM	4-9-1	98.26	97.23	95.56	97.28	98.23	91.99	94.62	91.78	95.36	91.69	97.29	95.62	94.78	93.45
LM	4-10-1	98.76	96.78	95.99	95.23	97.62	90.68	93.26	90.78	94.78	92.59	94.44	94.78	96.47	94.89
LM	4-11-1	97.99	97.99	96.39	92.89	97.23	92.73	91.09	93.69	91.99	93.69	94.59	96.78	95.23	92.99
RP	4-5-1	98.23	98.06	99.08	91.78	93.26	92.69	96.28	94.01	96.88	95.78	98.89	95.29	98.72	94.39
RP	4-6-1	98.65	95.69	97.69	96.25	94.28	90.88	95.78	93.65	93.89	96.19	97.48	94.88	96.48	94.96
RP	4-7-1	99.14	94.78	98.07	93.72	95.08	90.70	94.99	92.99	92.74	97.02	93.48	95.38	95.48	92.99
RP	4-8-1	97.69	97.58	94.67	92.22	91.09	91.29	93.69	91.99	89.99	96.78	89.98	94.81	94.62	93.46
P	4-9-1	97.12	96.69	92.69	91.11	91.69	92.39	92.68	90.28	88.69	95.28	88.28	89.62	92.78	94.86
RP	4-10-1	95.69	98.12	98.04	96.66	92.89	93.39	95.62	92.37	87.52	96.89	92.57	89.88	93.48	94.29
RP	4-11-1	99.74	93.39	92.26	96.28	93.66	90.88	94.78	91.73	98.72	97.86	93.58	91.29	96.49	95.06
BFGS	4-5-1	95.59	96.27	95.78	95.55	94.69	89.26	96.45	92.68	97.59	94.72	94.78	95.38	95.78	93.78
BFGS	4-6-1	96.99	91.99	94.37	94.44	95.61	88.16	93.69	93.33	94.63	96.19	95.38	94.80	96.18	91.11
BFGS	4-7-1	98.76	96.09	98.78	93.39	93.78	88.23	95.85	94.08	93.78	95.89	96.48	95.99	97.28	90.79
BFGS	4-8-1	99.03	96.79	96.78	97.01	95.29	88.92	96.69	92.99	95.85	97.48	96.17	96.30	96.18	92.86
BFGS	4-9-1	98.89	97.77	95.78	96.06	93.78	87.79	97.26	93.99	92.79	93.89	95.27	89.99	94.49	94.99
BFGS	4-10-1	97.66	98.07	94.23	95.29	97.28	86.29	93.69	91.28	91.99	92.59	96.47	89.96	93.18	93.49
BFGS	4-11-1	98.99	96.08	96.78	94.24	94.09	85.29	94.99	92.78	96.45	94.89	94.61	88.99	88.96	95.89

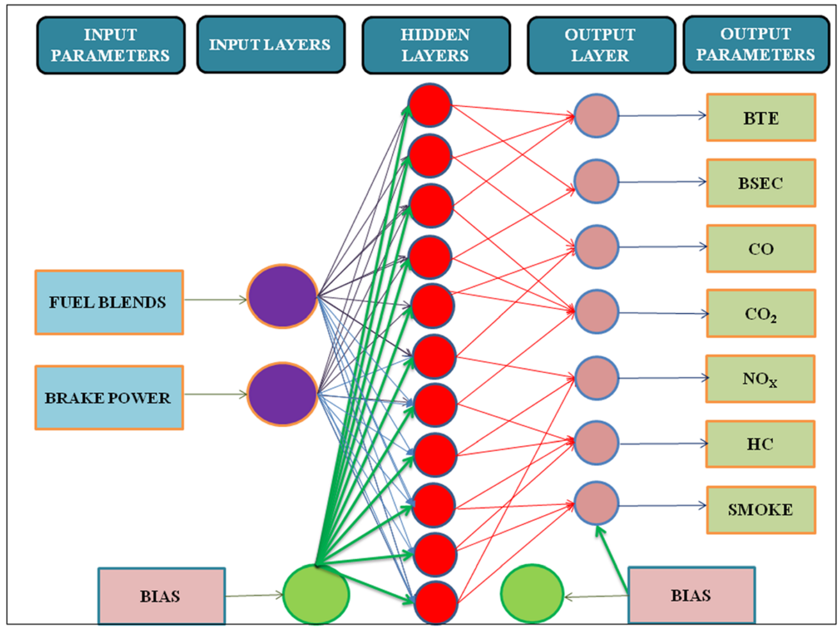

Fig. 1 Configuration of an ANN model

Total uncertainty

= √{(total performance deeds) 2 + (total emission deeds) 2}
= √{(UCBTE) 2 + (UCBSEC) 2 + (UCHC) 2 + (UCCO) 2
+ (UCNOx 2 + (UCsmoke) 2}
= √{(0.5) 2 + (0.7) 2 + (0.4) 2 + (0.14) 2 + (0.7) 2 + (0.7) 2}
= ±1.378

NN model

The human brain consists of a very complex neural network which is used to change, withstand, decide and correlate human's decisive thoughts. The neural network of the human brain can be functionally similar when compared to ANN technique (Selvan et al. 2018a). This

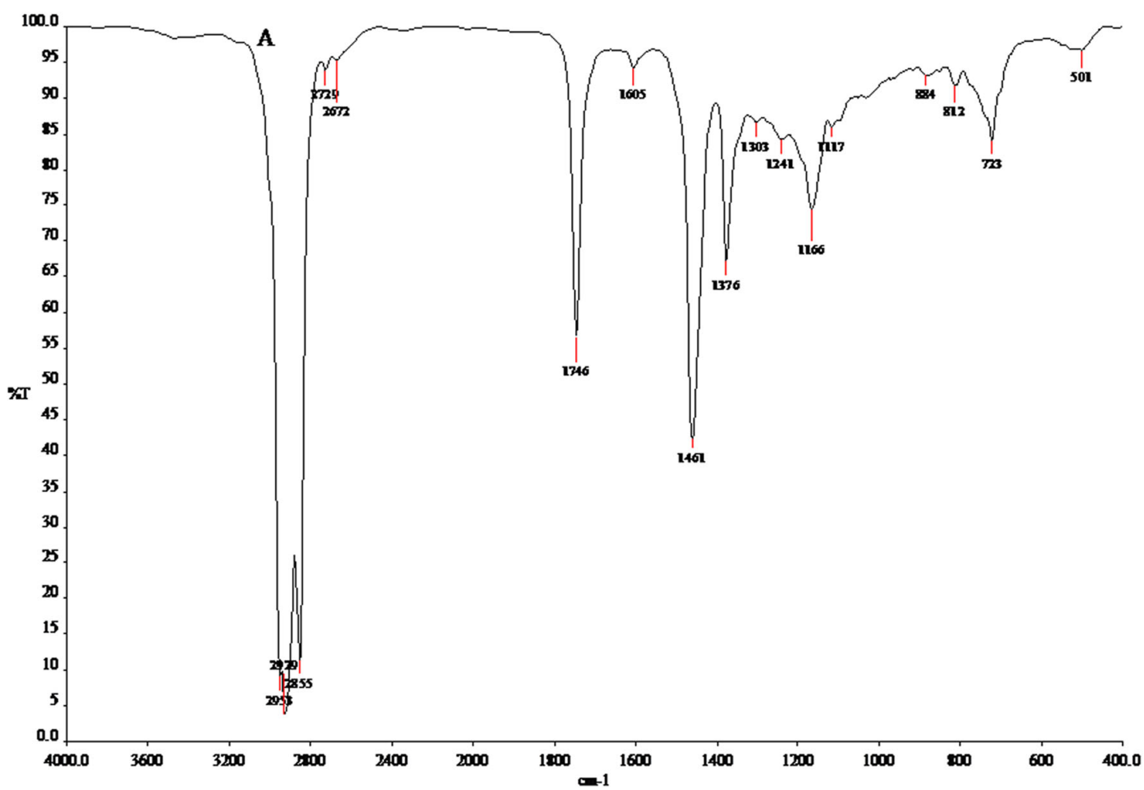

Fig. 2 FT-IR for citronella oil

Fig. 3 FT-IR for *Cymbopogon flexuous* oil

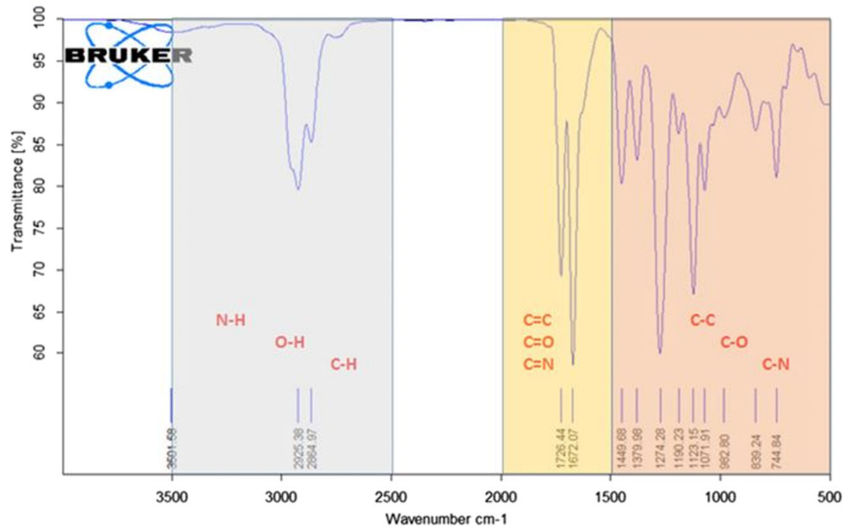

technique is used to inspect, simplify and additionally identify the inestimable number of parameters. The ANN is characterised with many neurons that are linking patterns for layers and transfer functions and can be more appropriately concealed as a magnitude of neurons (Selvan et al. 2018b). The hidden layers are connected to outer layers which represent synaptic weights; besides that, it is designed to minimise the performance function by using MSE (Wang and Gao 2018). Mentioned MSE has features that magnify convexity, regularity and differentiability and has an outstanding performance in the background of operation. The selection of learning algorithm to identify the transfer function plays a key role in ANN; there are many different algorithms available for the selection of the transfer function; these are SCG, LM, RP and BFGS. For a succeeding assortment of the transfer function, it is essential to select the learning algorithm. The examination for the selection of the best algorithms identified SCG, SCG, LM, LM, RP, LM for BTE, BSEC, CO, CO_2, HC, NO_x correspondingly. The neural network

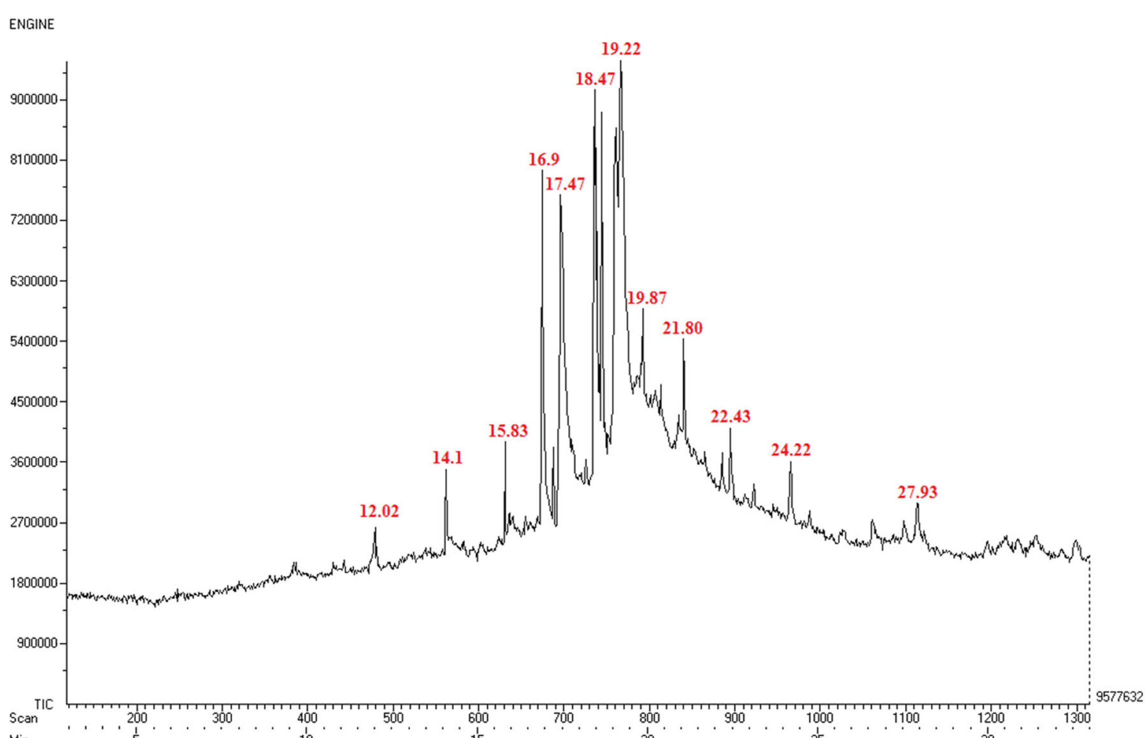

Fig. 4 GC-MS for citronella oil

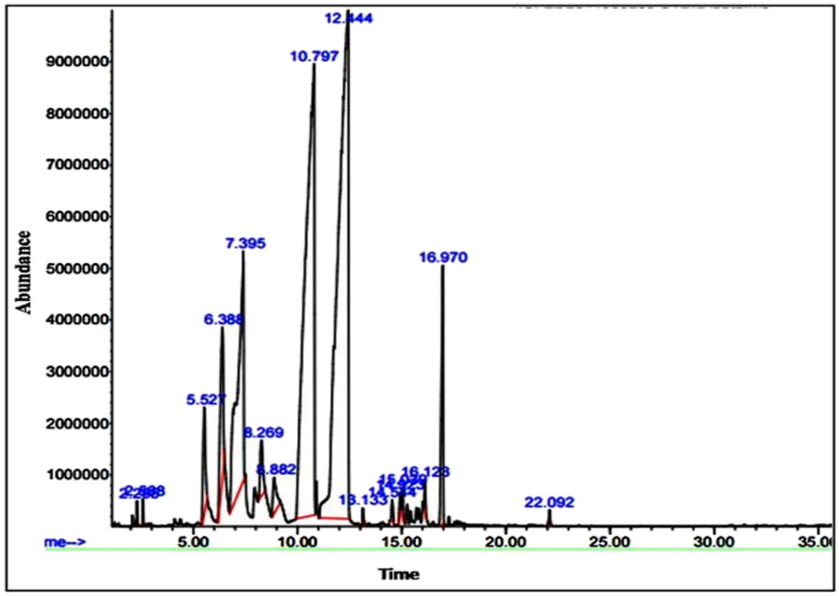

Fig. 5 GC-MS for *Cymbopogon flexuous* oil

Table 7 Chemical compounds present in citronella oil

S.no	Chemical Compound	Formula	Area (%)	Structure	IUPAC name (international union of pure and applied chemistry)
1	Citronellal	$C_{10}H_{18}O$	51.5	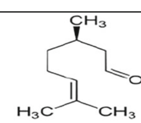	3,7-dimethyloct-6-en-1-al
2	Geranial	$C_{10}H_{18}O$	15	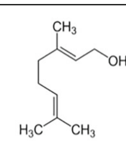	3,7-Dimethyl-2,6-octadien-1-ol
3	Citronellal	$C_{10}H_{20}O$	12.8	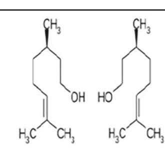	3,7-Dimethyloct-6-en-1-ol
4	Limonene	$C_{10}H_{16}$	4.7	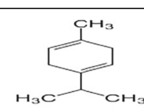	1-Methyl-4-(prop-1-en-2-yl)cyclohex-1-ene
5	Germacrene D	$C_{15}H_{24}$	2.5	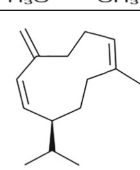	8-isopropyl-1-methyl-5-methylenecyclodeca-1,6-diene

Table 8 Chemical compounds present in *Cymbopogon flexuous* oil

S.no	Chemical Compound	Formula	Area (%)	Structure	IUPAC name (international union of pure and applied chemistry)
1	Neral (Citral-b)	$C_{10}H_{16}O$	30.1	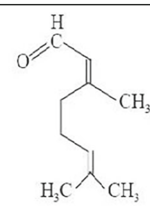	3,7-dimethylocta-2,6-dienal
2	Geranial (Citral-a)	$C_{10}H_{18}O$	33.1	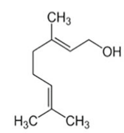	3,7-Dimethyl-2,6-octadien-1-ol
3.	Geranyl acetate	$C_{12}H_{20}O_2$	12.0	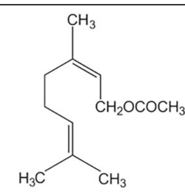	3,7-dimethylocta-2,6-dienyl acetate
4.	Citronellyl acetate	$C_{12}H_{22}O_2$	4.2	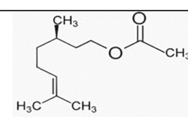	3,7-dimethyloct-6-enyl acetate
4	Limonene	$C_{10}H_{16}$	2.0	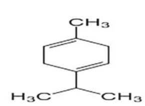	1-Methyl-4-(prop-1-en-2-yl)cyclohex-1-ene
5	Germacrene D	$C_{15}H_{24}$	2.5	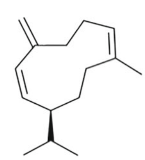	8-isopropyl-1-methyl-5-methylenecyclodeca-1,6-diene

structure for these parameters was found to be 4-11-1, 4-11-1, 4-7-1, 4-7-1, 4-11-1, 4-11-1 and 4-11-1 correspondingly and was tabulated as shown in Table 6.

Seventy percent of the randomly selected experimental data was cross validated with 15 % of the data and the remaining 15% of the data were used to examine the performance of the trained network. Consideration of the regression co-efficient (R^2) is used to predict the performance of ANN models. The proposed models of many researchers were framed according to MSE,

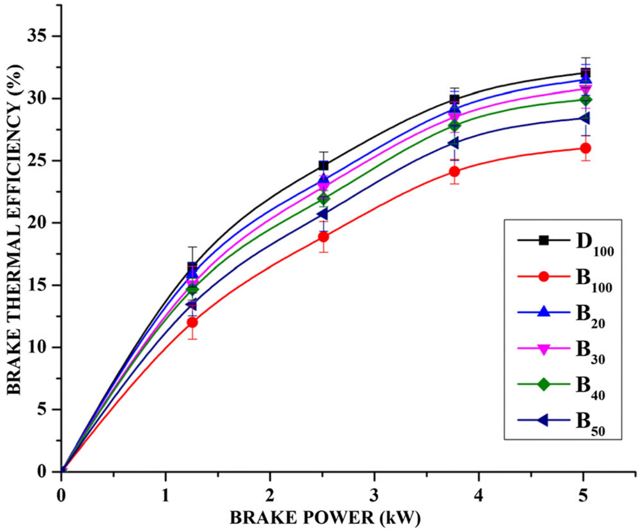

Fig. 6 Brake thermal efficiency vs. brake power

RMSE and MAPE; the values are utilised to develop the ANN model. The regression co-efficient (R^2) and the values used for developing the ANN model is calculated by the base equations represented below

$$R^2 = 1 - \frac{\sum_{i=1}^{n} (Ti - Oi)^2}{\sum_{i=1}^{n} Oi^2} \tag{5.1}$$

$$MAPE = \left\{ \frac{100}{n} \sum_{i=1}^{n} \left(\frac{Ti - Oi}{Oi} \right) \right\} \tag{5.2}$$

$$MSE = \frac{1}{n} \left\{ \sum_{i=1}^{n} \left((Ti - Oi)^2 \right) \right\} \tag{5.3}$$

$$RMSE = \sqrt{\frac{1}{n} \sum_{i=1}^{n} (Ti - Oi)^2} \tag{5.4}$$

The study is evaluated using numerical standard indicators with the values of R, MSE and MAPE. These measures decide the continuation or termination of the iterations. If the value of R is more than 0.98, MSE and MAPE values will be lesser than 0.001 and 5% accordingly, the iteration of the ANN model will be terminated. If these values are not achieved the termination will occur at 100th loop iteration. The ANN model is used to evaluate the engine performance and emission characteristics. Two input parameters were considered to develop the ANN model and 7 outputs were derived inclusive of HC, CO, CO2, NO_x and smoke opacity (emission parameters) and BTE and BSFC (performance parameters) as shown in Fig. 1.

Table 9 performance output response for different test fuels

BP	Diesel	B100	B20	B30	B40	B50
Brake thermal efficiency (%)						
0	0	0	0	0	0	0
1.256	16.4606	12.01	15.88878	15.09	14.67582	13.46
2.512	24.60314	18.87	23.4685	22.89	21.9506	20.71
3.768	29.90952	24.12	29.16162	28.51	27.81961	26.44
5.024	32.0498	26.01	31.50091	30.75	29.90997	28.42
Brake specific energy consumption (g/kW-h)						
1.256	23.0606	32.41	26.87582	25.38878	31.5675	31.78
2.512	14.60314	24.52	19.36031	17.8685	22.85213	23.12
3.768	12.30952	19.12	15.31961	13.56162	17.28765	18.12
5.024	11.7498	17.69	13.00091	14.70997	15.70997	16.49

Table 10 Emission output response for different test fuels

BP	Diesel	B100	B20	B30	B40	B50
Carbon monoxide emission (g/kW-h)						
0	1.5	1.3	1.07	1.02	0.95	0.89
1.256	1.21	1	0.88	0.75	0.62	0.52
2.512	1	0.841	0.63	0.61	0.48	0.42
3.768	0.85	0.79	0.58	0.46	0.4	0.31
5.024	2.92	2.75	2.34	2.236	2.13	2.025
Hydro carbon emission (g/kW-h)						
0	0.09	0.082	0.073	0.062	0.051	0.04
1.256	0.11	0.099	0.085	0.072	0.059	0.046
2.512	0.126	0.101	0.099	0.089	0.079	0.07
3.768	0.24	0.225	0.19	0.165	0.152	0.135
5.024	0.26	0.242	0.23	0.191	0.184	0.157
Carbon dioxide emission (g/kW-h)						
0	99.01	95.78	106.12	109.16	112.39	116.15
1.256	214.5	209.67	229.04	233.53	237.69	240.55
2.512	324.96	318.99	342.78	346.27	347.99	349.71
3.768	452.54	448.87	486.25	491.05	493.86	496.97
5.024	587.09	580.96	614.29	619.08	624.08	634
Oxides of nitrogen (g/kW-h)						
0	1.8	1.9	1.95	2	2.1	2.2
1.256	2.5	2.52	2.55	2.6	2.7	2.9
2.512	3.2	3.25	3.3	3.4	3.5	3.6
3.768	3.9	3.95	4.01	4.1	4.3	4.5
5.024	4.6	4.75	4.9	5	5.2	5.4
Smoke opacity (%)						
0	10.5	10.2	9.7	9.5	8.9	7.8
1.256	36.5	33.5	26.9	25.8	24.12	23.76
2.512	49.2	46.1	30.3	29.1	27.82	26.01
3.768	61.5	58.7	44.4	43.01	41.76	40.07
5.024	72.5	70.01	64.5	63.01	61.97	60.09

Results and discussion

Results of FT-IR

The very forceful peak of C=O band extended for citronella oil emerged at the wavelength province of 1740

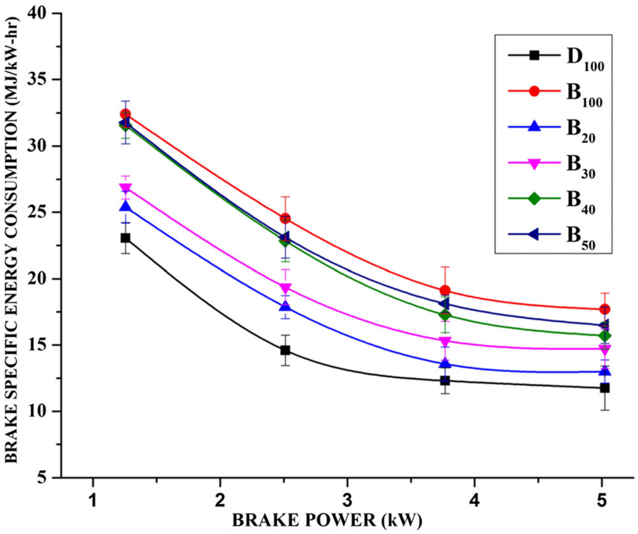

Fig. 7 Brake specific energy consumption vs. brake power

and 1724 cm^{-1}; mainly, these bands are usually from fatty acids and fatty esters and the average peak of C–O bands emerge at the wavelength province of 1377, 1233, 1196, and 1155 cm^{-1}; predominantly, medium bonds of esters are within the limit of about 1400 to 1000 cm^{-1}. From the examination of spectrum peaks, –OH band extended was exposed to be at a range of 3380 cm¯1; CH_2 and CH_3 peak bonds are exposed at the range of 2965–2924 cm^{-1}, as exposed in Fig. 2.

Figure 3 represents the FT-IR of extracted *Cymbopogon flexuous* oil, the peak inclusion of the OH band indicates that phenolic compounds emerged at a frequency of 2923 cm^{-1}. The powerful peak of C=O band extended for *Cymbopogon flexuous* oil emerged at the wavelength province of 1726.44 cm^{-1}. The average peak C–O bands emerge at the wavelength province at 982.60 and 1672.07 cm^{-1}; predominantly, medium bonds of esters lie within the limit of about 900 to 1700 cm^{-1}.

Results of GC-MS

The GC-MS investigation was carried out at IITM, Chennai. These investigations were carried out to find the different chemical constituents present in citronella oil and *Cymbopogon flexuous* oil and their different peaks which are exposed in Figs. 4 and 5. Generally, the GCMS furnace drives with four dissimilar ramps to attain a target temperature. At first, the furnace starts with 50 °C which is held for 2 min. Following that, the first ramp started with 10 °C to reach 100 °C and is then held for 2 min. Again, the second ramp is initiated with 10 °C to attain 150 °C for a time of 2 min. Then, a third ramp is started with 5 °C to attain 200 °C held for 2 min. The last ramp is opened with 5 °C to attain a target temperature of 250 °C and is then held for 10 min. Finally, the oven and GC-MS system terminal temperatures were set at 250 °C. The system is attached to 60–600 ammo scanning range of the photomultiplier tube detector. The helium was the carrier gas employed in the system with the purity of 99.9% and the surge rate was 1 ml/min to sweep the vapour phase organic compound through the GC column. The term RT is briefed as time availed by the sample's compound present in the GC. Every compound has a different RT; it is based on their boiling point, column temperature, flow rate of carrier and length of column. Besides, the long column improves the separation and increase the column temperature and the carrier flow rate; they reduce the RT of the compound. In addition, the minimal boiling point of compounds has increased the vapour pressure of compounds and the higher molecular weight of compound resulted in higher RT (Ramalingam et al. 2019). The chemical analysis was conceded out with the help of the JEOL GC series system and employed the records match software to identify the peaks. The citronella oil and *Cymbopogon flexuous* oils include 35 to 40% of monoterpenes, 45 to 50% of sesquiterpenes, 1.5 to 3% of n-alkanes and 0.5 to 1% of unknown compounds. Generally, an increase in the length of n-alkane chain reduces the ignition lag period. In addition, double bonds in the n-alkane chain improve the lag period; the ignition lag also increases with the availability of aromatic content in the fuel mixture. The presence of oxygen content in the functional group of fuel mixture influenced the ignition lag period. The length of the hydrocarbon chain was used to calculate the energy content and the boiling point of the fuel. Moreover, an increase in the hydrocarbon chain length led to an increase in the energy content and boiling point. '1-Docosanol, acetate' reported a maximum RT of about 27.93 min. The major elements of hydrocarbon and oxygen molecules such as 'isopropyl stearate', 'docosanoic acid, methyl ester', 1-docosanol, acetate, 9-octadecenoic acid (Z), tetradecyl ester were acknowledged.

The compounds present in citronella oil and *Cymbopogon flexuous* oil were identified and compared with diesel mass spectra. The diesel has 75 compounds. High RT and peak area compounds are identified for diesel as n-tridecane, pentadecanen-tetradecane, hexadecane, n-hexadecane and 'isopropyl stearate', 'docosanoic acid, methyl ester', 1-docosanol, acetate are identified in citronella fuel. 1-Docosanol, acetate symbolises an alkane hydrocarbon and other compounds represent linear groups which are acknowledged as n-hexadecane, n-tridecane, pentadecanen-tetradecane and hexadecane. The citronella oil and *Cymbopogon flexuous* oil mainly hold alkanes and phenols. The alkanes are trouble-free for transport and highly flammable. In comparison, most properties of citronella fuel and *Cymbopogon flexuous* oil are similar to diesel as per the GC-MS report, numerous chemical constituents are present in both extracted citronella and *Cymbopogon flexuous* oils. Some of the major chemical compounds are exposed in Tables 7 and 8.

Table 11 Summary of statistical value for BTE, BSEC, CO, CO2, HC, NO_x and smoke using different training algorithms

Parameters	Learning algorithm	Network structure	Training set			Testing set		
			R	RMSE	MAPE	*R*	RMSE	MAPE (%)
BTE	SCG	4-11-1	0.9992	0.401	0.99	0.9965	0.405	1.15
	LM	4-11-1	0.9991	0.389	1.25	0.9952	0.459	2.15
	RP	4-5-1	0.9976	0.372	2.84	0.9931	0.526	2.38
	BFGS	4-10-1	0.9823	0.402	3.12	0.9960	0.428	3.12
BSEC	SCG	4-11-1	0.9998	0.019	0.65	0.989	0.026	0.87
	LM	4-8-1	0.9986	0.013	0.79	0.972	0.031	1.38
	RP	4-10-1	0.9972	0.021	0.83	0.979	0.038	2.89
	BFGS	4-8-1	0.9991	0.018	1.69	0.983	0.046	4.18
CO	SCG	4-9-1	0.9812	0.0200	2.38	0.9621	0.0228	3.89
	LM	4-7-1	0.9991	0.0201	2.18	0.9784	0.0206	3.17
	RP	4-5-1	0.9745	0.0189	2.54	0.9542	0.0399	4.10
	BFGS	4-5-1	0.9789	0.0179	3.09	0.9432	0.123	2.99
CO_2	SCG	4-5-1	0.976	0.0099	2.94	0.941	0.286	3.99
	LM	4-7-1	0.998	0.0151	1.82	0.955	0.0158	2.60
	RP	4-5-1	0.956	0.0139	3.08	0.948	0.0458	2.88
	BFGS	4-7-1	0.948	0.0128	1.99	0.896	0.0389	2.92
HC	SCG	4-9-1	0.9681	0.0154	3.29	0.9034	0.0996	4.58
	LM	4-7-1	0.9482	0.0168	2.89	0.8742	0.0648	4.37
	RP	4-11-1	0.9952	0.0182	2.48	0.9076	0.0195	4.26
	BFGS	4-8-1	0.9901	0.0159	4.01	0.8894	0.0784	4.84
NO_x	SCG	4-5-1	0.9894	2.318	2.35	0.9812	2.998	2.47
	LM	4-11-1	0.9919	2.459	0.89	0.9849	2.685	1.69
	RP	4-7-1	0.9689	2.999	1.89	0.9765	2.798	1.99
	BFGS	4-8-1	0.9789	2.267	2.98	0.9661	3.128	3.28
Smoke	SCG	4-5-1	0.9802	0.489	2.08	0.976	0.512	2.99
	LM	4-10-1	0.9758	0.512	1.89	0.990	0.489	2.84
	RP	4-11-1	0.9874	0.477	0.99	0.985	0.389	1.23
	BFGS	4-11-1	0.9992	0.189	0.65	0.993	0.333	0.98

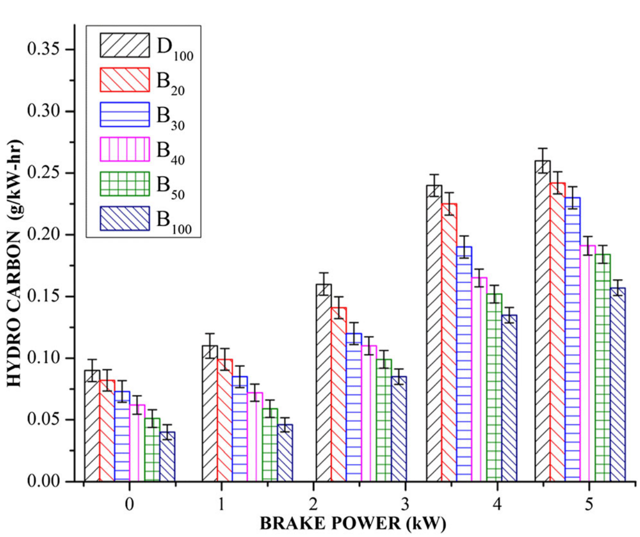

Fig. 8 Hydrocarbon emission vs. brake power

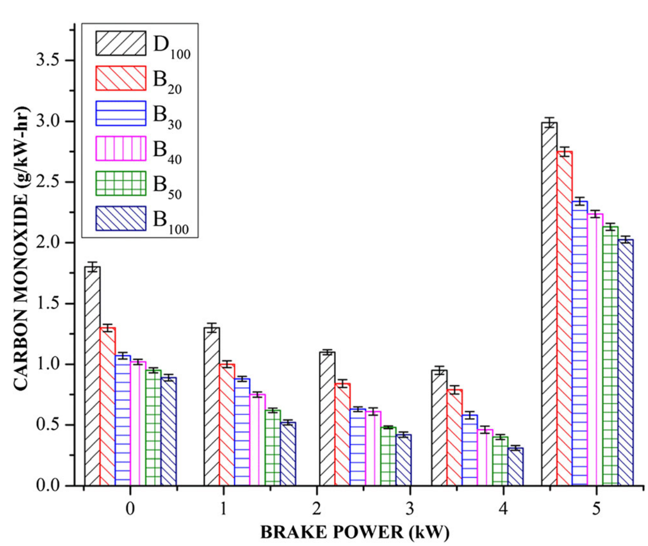

Fig. 9 Carbon monoxide emission vs. brake power

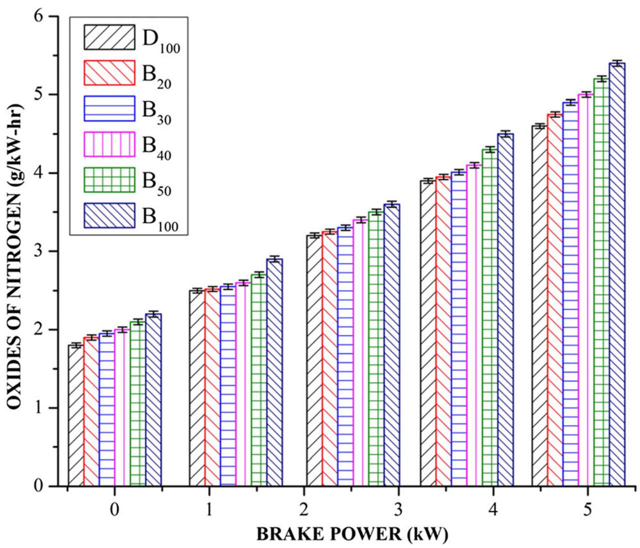

Fig. 10 Oxides of nitrogen emission vs. brake power]

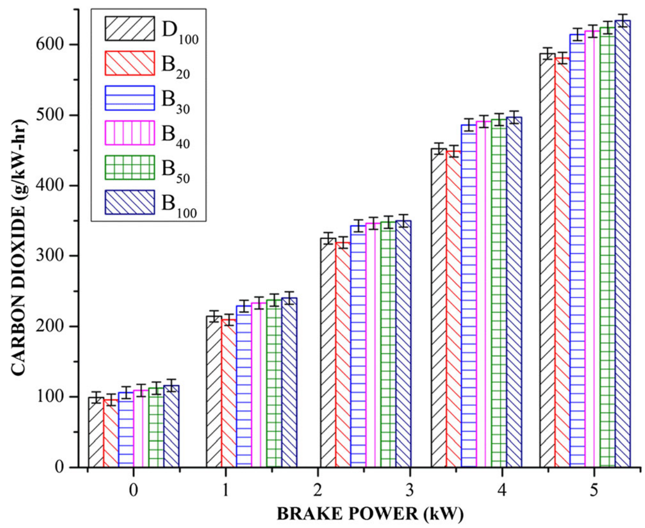

Fig 11 Carbon dioxide emission vs. brake power

Results of BTE vs. BP

The parameter of BTE is used to explore the engine capability to renovate the fuel source with heat energy into useful mechanical work. The chief constraints that have a major impact on the results of BTE are CV, CN, O_2 and kinematic viscosity at hand in the fuel (Subramani et al. 2018). Figure 6 exemplifies the discrepancy of the BTE for biofuel-diesel with the diverse percentage of C50CF50 biofuel at assorted engine BP. From the result, it is perceptible that BTE increases for 20% biofuel blended with diesel, followed by a decrease beyond the addition of 20% biofuel blended with diesel, and that may be the reason of minimal CV and SFC. The highest BTE is 32.04% for diesel which is 0.54% higher than B20 (31.50%). The BTE for B20, B30, B40, B50 and B100 blend are 31.50%, 30.75%, 29.91%, 28.42% and 25.05% respectively (Tables 9 and 10). These annotations are unfailing with Dhinesh et al. (2017). He established that *Cymbopogon flexuosus* biofuel had poor BTE when correlated with diesel, which may be ascribed to poor evaporation and low CV. CV of biofuel blend may be the reason for the heavy amount of O_2 content and density. The following equation was used to compute the BTE.

$$BTE = \frac{BP}{TFC \times CV} \ (\%) \tag{6}$$

$$BP = \frac{2\pi NT}{60} \ 0S \ \ (kW) \tag{a}$$

$$TFC = \ \frac{\rho \times \nu}{t} \ \ (g/s) \tag{b}$$

Results of BSEC vs. BP

The constraint BSEC is defined as the energy acquired by flaming of fuel for 1 h; in other words, quantity of energy consumed by engine to produce per kW power (Ramalingam et al. 2018). Figure 7 exemplifies the discrepancy of the BSEC for biofuel-diesel with the diverse percentage of C50CF50 biofuel at assorted engine BP. The chief constraints that have a major impact on the result of BSEC are CV, CN, O_2 and kinematic viscosity (Vigneswaran et al. 2018). The least BSEC is 11.74 MJ/kW-h for diesel that is 10% lower than for B20 (13.009 MJ/kW-h). The BSEC for B20, B30, B40, B50 and B100 blend is 13.009 MJ/kW-h, 14.70 MJ/kW-h, 15.71 MJ/kW-h, 16.49 MJ/kW-h and 17.69 MJ/kW-h respectively at the high load state. These annotations are unfailing with the results of Sathiyamoorthi and Sankaranarayanan (2017), who established that the lemongrass biofuel has higher BSEC when correlated with diesel. This may be the reason for minimal CV and lower volatility. The following equation was used to compute the BSEC. In addition, Table 11 shows the performance output response for the different test fuels.

$$BSEC = \frac{TFC \times 3600}{BP} \times CV \ \ (MJ/kW{-}hr) \tag{6.2}$$

Results of HC vs. BP

Generally, the quantity of HC in the tailpipe exhaust is based on fuel property, injection condition, engine working conditions, spray condition and the communication between air/fuel ratio in the engine (Dhinesh et al. 2018). Figure 8 exemplifies the discrepancy of the HC for biofuel-diesel with the diverse

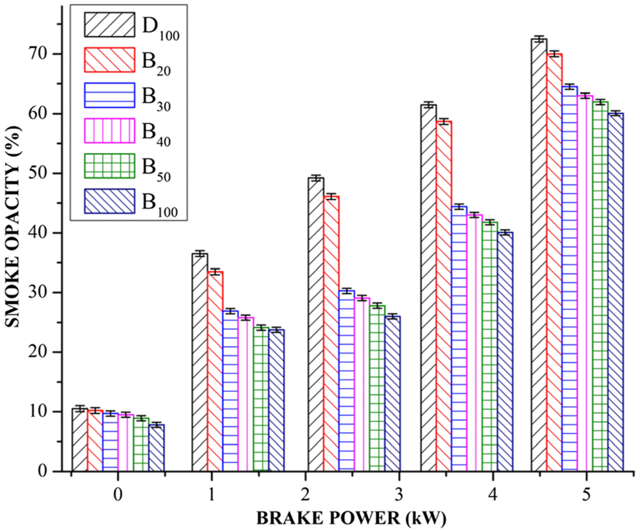

Fig. 12 Smoke emissions vs. brake power

percentage of C50CF50 biofuel at assorted engine BP. The amount of HC in tailpipe exhaust has risen with increasing engine load due to a reduction in volumetric efficiency and higher fuel accumulation. It is apparent that diesel emits more HC when correlated with biofuel blends this may be ascribed to a lack of O_2 content in the diesel. On the other hand, the entire biofuel blend had lower HC owing to higher O_2 availability in the blend. It is also noticed that biofuel blend has higher HC emission reduction only at low and middle load states. It may be ascribed to greater mixing, evaporation rate and fulfilling the time required for complete burning. The HC is 0.26 g/kW-h for diesel that is 40% higher than B50 (0.157 g/kW-h). The HC for B20, B30, B40, B50 and B100 are 0.23 g/kW-h, 0.191 g/kW-h, 0.184 g/kW-h, 0.157 g/kW-h and 0.242 g/kW-h respectively at the maximal load state. These annotations are unfailing with Purushothaman and Nagarajan (2009a). He established that neat orange biofuel has lower HC when correlated with diesel. In addition, surface tension and viscous property of fuel play an imperative role in mixing and atomization progress, since neat orange oil has a similar viscous property to diesel. They accelerate the fine droplet in size, rapid evaporation and abundance availability of O_2 leading to complete fuel burning inside the cylinder thus curbing HC emissions.

Results of CO vs. BP

The CO emissions are mainly formed in the fuel-rich zone due to a shortfall of O_2 or air in the chamber, which is only an intermediate zone product. CO is a colourless, smell-less and poisonous gas (Parthasarathy et al. 2016). Figure 9 exemplifies the discrepancy of CO for biofuel-diesel with the diverse percentage of C50CF50 blend at assorted engine BP. It is apparent that the CO value diminishes with the increase in engine BP up to a 70% load state; beyond that, it is drastically increased. This may be ascribed to the increase in fuel fraction, in-cylinder temperature, knocking capability and lack of O_2 at extreme BP which leads to incomplete combustion. Diesel emits more CO when correlated with biofuel blends; it may be attributed to a lack of O_2 content in the diesel. The CO is 2.92 g/kW-h for diesel which is 44% higher than B50 (2.025 g/kW-h) The CO for B20, B30, B40, B50 and B100 blends is minimal than diesel by 2.34 g/kW-h, 2.236 g/kW-h, 2.13 g/kW-h, 2.025 g/kW-h and 2.75 g/kW-h respectively at a maximal load state. These annotations are unfailing with Anand et al. (2010). They established that turpentine oil biofuel has lesser CO, which may be the reason for higher O_2 presence which leads to proper combustion. Besides that, the CI engine employed with any sort of oxygenated fuel such as biofuel, methyl ester, better viscous fuel and alcohol reduces the CO enrichment which is exposed by numerous researchers.

Results of NO_x vs. BP

Generally, there is a non-uniform distribution of fuel in diesel engines, which leads to high in-cylinder temperature. The NO_x formation mainly occurs at high temperature. In the high in-cylinder temperature region, the

Table 12 Summary of R, RMSE and MAPE for BTE, BSEC, CO, CO2, HC, NO_x and smoke using different training algorithms

Output parameters	Training algorithm	No. of neurons in hidden layers	*R* (Pearson's product moment correlation)	RMSE (root mean squared error)	MAPE (mean absolute percentage error)
BTE	SCG	11	0.9965	0.405	1.15
BSEC	SCG	11	0.989	0.026	0.87
CO	LM (LevenbergeMarquardt)	7	0.9784	0.0206	3.17
CO2	LM (LevenbergeMarquardt)	7	0.955	0.0158	2.60
HC	RP	11	0.9076	0.0195	4.26
NO_x	LM (LevenbergeMarquardt)	11	0.9849	2.685	1.69
Smoke	BFGS	11	0.993	0.333	0.98

NO_x is produced by the reaction between nitrogen and oxygen. The NO_x formation rate increases in the regions which are close to the stoichiometric operating condition (Vallinayagam et al. 2015). Figure 10 exemplifies the discrepancy of the NO_x for biofuel-diesel with the diverse percentage of C50CF50 biofuel at assorted engine BP. It is apparent that diesel emits lower NO_x when correlated with biofuel blends except for B100; this may be credited to the lack of O_2 content in diesel. On the other hand, the whole biofuel blend had higher NO_x when correlated with diesel due to higher O_2 content present in biofuel blend which leads to an increase in peak combustion temperature. The NO_x emission of biofuel blend increases with the rise in engine load owing to rapid combustion, heat energy of the previous cycle and O_2 availability. Beyond that, the B20 blend observes a reduction in NO_x emission outcome owing to a lesser heating value of the blend. The NO_x is 4.6 g/kW-h for diesel which is 15% lower than B50 (5.4 g/kW-h) The NO_x emissions for B20, B30, B40, B50 and B100 blends are 4.9 g/kW-h, 5 g/kW-h, 5.2 g/kW-h, 5.4 g/kW-h and 4.75 g/kW-h respectively. These annotations are unfailing with the results of Anandavelu et al. (2011), who established that eucalyptus oil biofuel has higher NO_x when correlated with diesel, which may be credited to higher O_2 presence. In addition, higher adiabatic flame temperatures majorly influence the formation of NO_x. Generally, the biofuel blend has greater

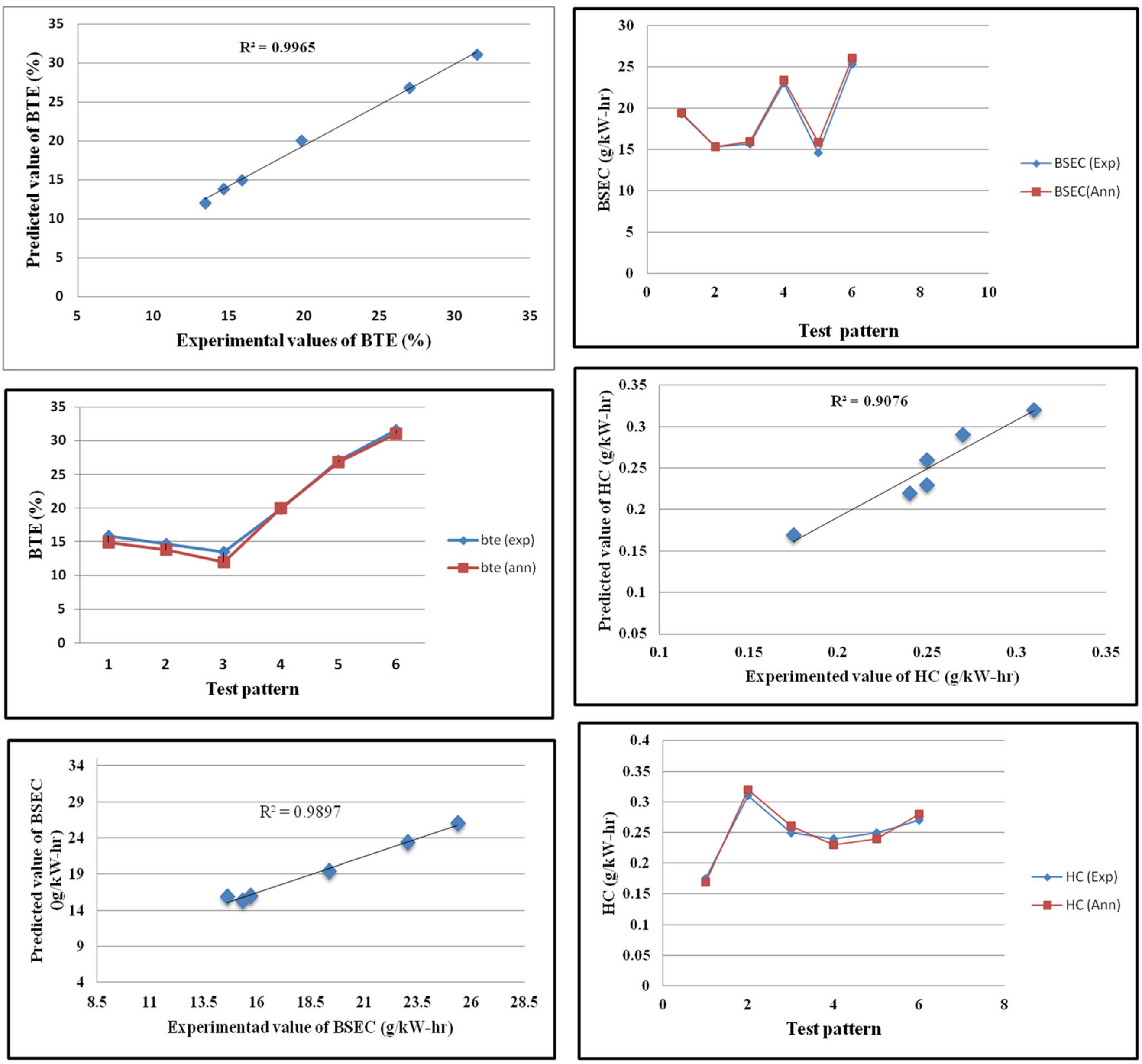

Fig. 13 The contrast between the ANN predictions and experimental results

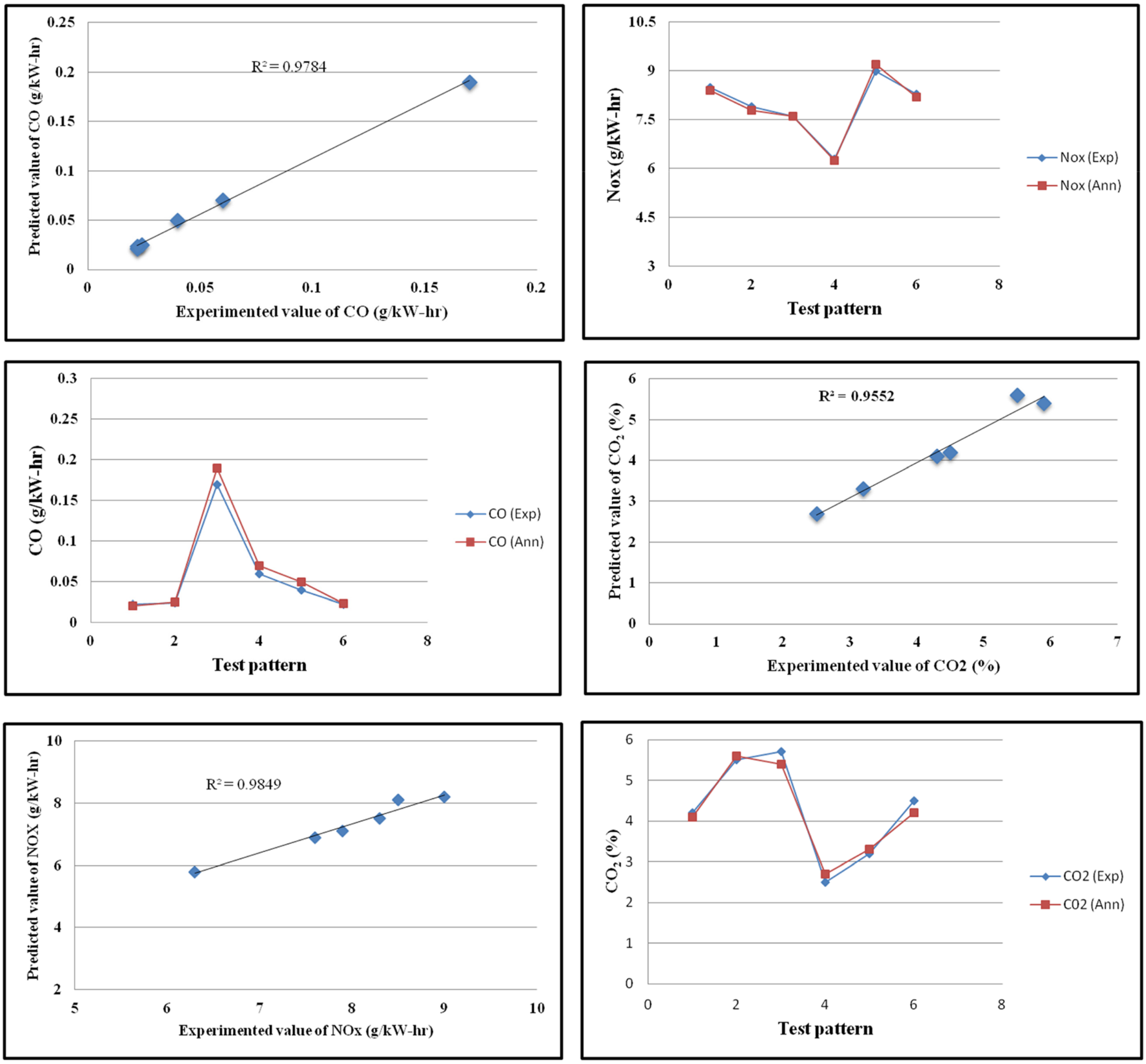

Fig. 13 (continued)

unsaturated fatty content. This may be contributing to the higher adiabatic flame temperature.

Results of CO_2 vs. BP

One of the primary sources of greenhouse gas (GHG) emission is CO_2 which is a result of complete combustion (Dhinesh et al. 2017). It is an important resource for the growth and photosynthesis of plants and trees. Carbon atoms are released during the combustion of fossil fuels which leads to the increase of CO_2 in the atmosphere; but during combustion of biofuel, the CO_2 that is released does not increase the CO_2 in the atmosphere; rather, it is recirculated, as biofuel is produced from plants and trees (Manigandan et al. 2019a). Figure 11 exemplify the discrepancy of the CO_2 for biofuel-diesel with the diverse percentage of C50CF50 biofuel at assorted engine BP. It is apparent that diesel emits higher CO_2 when correlated with biofuel blends except B20; this may be reason for complete combustion. On the other hand, the B20 blend had higher CO_2 except when correlating with diesel due to a higher quantity of oxygen bound in B20 biofuel blend; it significantly promotes complete combustion but other blends had lower CO_2 owing to a higher fraction of biofuel content resulting in improper atomization, which leads to incomplete combustion. The CO_2 is 587.09 g/kW-h for diesel that is 7.4% lower than B50 (634

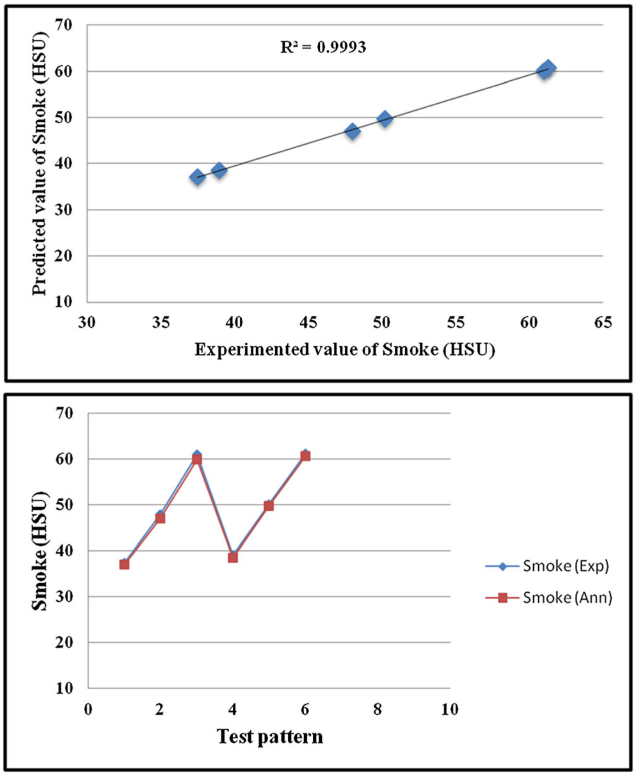

Fig. 13 (continued)

g/kW-h). The CO_2 emissions for B20, B30, B40, B50 and B100 blends are 614.29 g/kW-h, 619.08 g/kW-h, 624.08 g/kW-h, 634 g/kW-h and 580.96 g/kW-h respectively at the full load state. These annotations are unfailing with the results of Karthikeyan and Mahalakshmi (2007). He established that the turpentine biofuel has higher CO_2 when correlated with diesel which may be credited to a higher abundance of O_2. However, 100% of turpentine oil has drastically lowered CO_2 owing to higher density and lower heating energy. The current investigation has also recognised a similar fact owing to inherent O_2 and better viscous property of test fuel that speed up the superior combustion resulting in higher CO_2 emissions.

Results of Smoke vs. BP

The formation of smoke mainly depends on the amount of O_2 present in test fuel (Uyumaz 2018). In other words, fuel composition is directly related to the smoke emission (Li et al. 2015). Figure 12 exemplifies the discrepancy of the smoke for biofuel-diesel with the diverse percentage of C50CF50 biofuel at assorted engine BP. The amount of smoke opacity in tailpipe exhaust rises with increasing the load, which can be clearly seen at the top load state. It is apparent that the diesel emits more smoke when correlated with biofuel blends; this may be credited to the lack of O_2 content in the diesel. On other hand, the entire biofuel blend had lower smoke when correlated with diesel due to a deficiency of aromatic content, lesser C/H proportion and higher O_2 which improves combustion and fuel oxidation. The smoke is 72.5% for diesel that is 17.11% higher than B50 (60.09%). The smoke for B20, B30, B40, B50 and B100 are 64.5%, 63.01%, 62%, 60% and 70% respectively at the full load state. These annotations are unfailing with Kumar et al. (2018); He established that the lemon peel oil blend has inferior smoke when correlated with diesel, which may be credited to higher O_2 presence, better fuel burning rate and better volatility of fuel.

Conversion of g/kW-h

The exhaust gas emissions (CO, HC, CO_2 and NO_x) are calculated in PPM and converted into g/kW-h as per the canonical testing procedure. In addition, Table 12 shows the emission output response for different test fuels.

Prediction of engine behaviour using the ANN model

In the present prediction work, nonlinear problems are predicted using ANN models. The model is used to identify the engine performance and emission constraints when energised with combination of two low viscous oil and its blend namely B20 (10% lemongrass oil + 10% citronella oil + 80% diesel), B30 (15% lemongrass oil + 15% citronella oil + 70% diesel), B40 (20% lemongrass oil + 20% citronella oil + 60% diesel), B50 (25% lemongrass oil +25% citronella oil +50% diesel) and B100 (50% lemongrass oil +50% citronella oil). The developed ANN model has a trouble-free, reliable character and toolboxes available to acquire precise prediction results.

The developed MATLAB network has two inputs namely fuel blend and brake power and the chosen seven output parameters are NO_x, CO, HC, CO_2, smoke, BTE and BSEC. The modelled network for prediction in diesel engine energised with a novel combination of two low viscous biofuels and its blend is based on the test run data. In the developed model, a totality of 30 test patterns was employed to test the efficiency of the model, wherein 80% of the test patterns (24 patterns) were randomly selected and employed for training, whereas the remaining 20% (6 patterns) have been assigned for testing and validation

It is a necessity to choose the optimal learning algorithms and hidden neuron (HN) number to guarantee the developed network (Mostafa et al. 2019). In this prediction study, the optimal learning algorithms of architecture and numbers of HN were decided and followed by numerous trial and error tests on the basis of MSE results and R value report. Generally, an increased value of R and a reduced value of MSE decides the optimum value of a number of HN and learning algorithms in a neural network. In this present prediction study, the value of R and RMSE has been found as the maximum and minimum values respectively, and from these values, it is decided that LM learning algorithms and eleven numbers of hidden neurons is the most optimal solution and was tabulated in Tables 9 and 10. The contrast between the ANN predictions and experimental results are established in Fig. 13.

The R value for the BTE, BSEC, CO, CO_2, HC, NO_x and smoke is found to be 0.9965, 0.989, 0.9784, 0.955, 0.9076, 0.9849 and 0.993 respectively, whereas the RMSE value for the BTE, BSEC, CO, CO_2, HC, NO_x and smoke is found to be 0.405, 0.026, 0.0206, 0.0158, 0.0195, 2.685 and 0.333 respectively. It should be marked that the value of RMSE indicates the error throughout the learning process. The value MAPE for the BTE, BSEC, CO, CO_2, HC, NO_x and smoke is identified as 1.15%, 0.87%, 3.17%, 2.6%, 4.26%, 1.685% and 0.979% correspondingly.

The present developed ANN model predicts that relative error is less than 4% which was within the range of satisfactory level. According to the error analysis, it is matching the data predicted by ANN and experimental analysis. In addition to the data present in the Table 10, the R value is ranging between 0.9076 and 0.9965, whereas MAPE values are ranging between 0.98 and 4.26%. which is very small. The developed ANN model is obviously an effective tool and it has an excellent capability to foretell the performance and emission parameters of the engine that were very near to experimental results.

The researcher highlighted and informs that the ANN model effectively minimises experimental cost, experimentation time and complexity of experimental analysis and this type of prediction model is more beneficial for engine output response mapping and also supports the control system (Wang and Gao 2018).

Conclusion

This study analytically and experimentally evaluated the effectiveness of conventional diesel engine powered with a novel combination of lemongrass and citronella biofuel with diesel and its blends. The examination fuel organised by merging of L50C50 biofuel with diesel at five diverse fractions (i.e. 20, 30, 40, 50 and 100 vol%), and the prepared blends are called B20, B30, B40, B50 and B100 respectively.

- The B20 blend exhibits improved performance outputs for BTE and BSEC than other biofuel blends by 31.5% and 13.009 MJ/kW-h. In addition, the exhaust emission output response was greatly greener for the B20 blend compared with conventional diesel. It is a proof from the result HC, CO and smoke by 0.23 g/kW-h, 2.34 g/kW-h and 64.5% respectively. On the whole, the addition of C50CF50 fuel in diesel exhibits better emission reduction apart from NO_x emission.
- The developed ANN network was employed to predict both performance and emission output responses and provided admirable outcomes, by which the value of R is elevated to 97% for all output constraints. Besides, the accurateness of the ANN model is also greater, and the high R values range between 0.9076 and 0.9965 and the low MAPE values range between 0.98 and 4.26%. It is apparent that the developed model is an effective tool and it has an excellent capability to predict the engine effectiveness and issuing the results that were very near to experimental results.

Acknowledgements One of the authors, Mr. Krishnamoorthy, state his extended thanks to ACRF for granting fellowship, and also, the researchers are conveying their hearty thanks to the Department of Automobile, MIT, Anna University, Chromepet, Chennai 44.

Funding information This study was financially supported by ACRF.

Abbreviations CI, compression ignition; CV, calorific value; CN, cetane number; CO, carbon monoxide; NO_x, oxides of nitrogen; CO_2, carbon dioxide; HC, hydrocarbon; BSEC, brake specific energy consumption; BTE, brake thermal efficiency; ASTM, American Society for Testing and Materials; BP, brake power; ANN, artificial neural network; HSU, Hartridge smoke units; LGO, lemongrass oil; WCO, waste cooking oil; GC-MS , gas chromatography-mass spectrometry; FT-IR , Fourier transform infrared spectroscopy; MSE, mean square error; MAPE, mean absolute percentage error

References

Alagumalai A (2015) Combustion characteristics of lemongrass (Cymbopogon flexuosus) oil in a partial premixed charge compression ignition engine. Alex Eng J 54:405–413. https://doi.org/10.1016/j.aej.2015.03.021

Amine M, Hadrich B, Kriaa K, Kechaou N (2018) Chemical engineering & processing : process intensification lab-scale extraction of essential oils from Tunisian lemongrass (Cymbopogon fl exuosus). Chem Eng Process Process Intensif 124:164–173. https://doi.org/10.1016/j.cep.2017.12.012

Anand BP, Saravanan CG, Srinivasan CA (2010) Performance and exhaust emission of turpentine oil powered direct injection diesel engine. Renew Energy 35:1179–1184. https://doi.org/10.1016/j.renene.2009.09.010

Anandavelu K, Alagumurthi N, Saravannan CG (2011) Experimental investigation of using Eucalyptus oil and diesel fuel blends in Kirloskar TV1 direct injection diesel engine. J Sustain Energy Environ 2:93–97

Ashok B, Nanthagopal K, Chaturvedi B, Sharma S, Thundil Karuppa Raj R (2018a) A comparative assessment on common rail direct injection (CRDI) engine characteristics using low viscous biofuel blends. Appl Therm Eng 145:494–506. https://doi.org/10.1016/j.applthermaleng.2018.09.069

Ashok B, Nanthagopal K, Saravanan B, Somasundaram P, Jegadheesan C, Chaturvedi B, Sharma S, Patni G (2018b) A novel study on the effect lemon peel oil as a fuel in CRDI engine at various injection strategies. Energy Convers Manag 172:517–528. https://doi.org/10.1016/j.enconman.2018.07.037

Ashok B, Thundil Karuppa Raj R, Nanthagopal K, Krishnan R, Subbarao R (2017) Lemon peel oil – a novel renewable alternative energy source for diesel engine. Energy Convers Manag 139:110–121. https://doi.org/10.1016/j.enconman.2017.02.049

Canakci M, Necati A, Arcaklioglu E, Erdil A (2009) Expert Systems with Applications Prediction of performance and exhaust emissions of a diesel engine fueled with biodiesel produced from waste frying palm oil. Expert Syst Appl 36:9268–9280. https://doi.org/10.1016/j.eswa.2008.12.005

Çay Y, Korkmaz I, Çiçek A, Kara F (2013) Prediction of engine performance and exhaust emissions for gasoline and methanol using artificial neural network. Energy 50:177–186. https://doi.org/10.1016/j.energy.2012.10.052

Devan PK, Mahalakshmi NV (2009) A study of the performance , emission and combustion characteristics of a compression ignition engine using methyl ester of paradise oil – eucalyptus oil blends. Appl Energy 86:675–680. https://doi.org/10.1016/j.apenergy.2008.07.008

Dharma S, Haji M, Chyuan H, Hanra A (2017) Experimental study and prediction of the performance and exhaust emissions of mixed Jatropha curcas-Ceiba pentandra biodiesel blends in diesel engine using arti fi cial neural networks. J Clean Prod 164:618–633. https://doi.org/10.1016/j.jclepro.2017.06.065

Dhinesh B, Annamalai M, Joshuaramesh I, Annamalai K (2017) Studies on the influence of combustion bowl modification for the operation of Cymbopogon flexuosus biofuel based diesel blends in a DI diesel engine. Appl Therm Eng 112:627–637. https://doi.org/10.1016/j.applthermaleng.2016.10.117

Dhinesh B, Bharathi RN, Joshuaramesh JI et al (2016a) An experimental analysis on the in fl uence of fuel borne additives on the single cylinder diesel engine powered by Cymbopogon fl exuosus biofuel. J Energy Inst:1–12. https://doi.org/10.1016/j.joei.2016.04.010

Dhinesh B, Isaac Joshua Ramesh Lalvani J, Parthasarathy M, Annamalai K (2016b) An assessment on performance, emission and combustion characteristics of single cylinder diesel engine powered by Cymbopogon flexuosus biofuel. Energy Convers Manag 117:466–474. https://doi.org/10.1016/j.enconman.2016.03.049

Dhinesh B, Maria Ambrose Raj Y, Kalaiselvan C, KrishnaMoorthy R (2018) A numerical and experimental assessment of a coated diesel engine powered by high-performance nano biofuel. Energy Convers Manag 171:815–824. https://doi.org/10.1016/j.enconman.2018.06.039

Dubey P, Gupta R (2018) Influences of dual bio-fuel (Jatropha biodiesel and turpentine oil) on single cylinder variable compression ratio diesel engine. Renew Energy 115:1294–1302. https://doi.org/10.1016/j.renene.2017.09.055

Dubey P, Gupta R (2017) Effects of dual bio-fuel (Jatropha biodiesel and turpentine oil) on a single cylinder naturally aspirated diesel engine without EGR. Appl Therm Eng 115:1137–1147. https://doi.org/10.1016/j.applthermaleng.2016.12.125

Ghobadian B, Rahimi H, Nikbakht AM, Najafi G, Yusaf TF (2009) Diesel engine performance and exhaust emission analysis using waste cooking biodiesel fuel with an artificial neural network. Renew Energy 34:976–982. https://doi.org/10.1016/j.renene.2008.08.008

Guedes AR, Reder A, De Souza C et al (2018) The Journal of supercritical Fluids Extraction of citronella grass solutes with supercritical CO 2 , compressed propane and ethanol as cosolvent : kinetics modeling and total phenolic assessment. J Supercrit Fluids 137:16–22. https://doi.org/10.1016/j.supflu.2018.03.003

Huang H, Liu Q, Shi C, Wang Q, Zhou C (2016) Experimental study on spray , combustion and emission characteristics of pine oil / diesel blends in a multi-cylinder diesel engine. Fuel Process Technol 153:137–148. https://doi.org/10.1016/j.fuproc.2016.07.016

Joy Prabu H, Johnson I (2015) Plant-mediated biosynthesis and characterization of silver nanoparticles by leaf extracts of Tragia involucrata, Cymbopogon citronella, Solanum verbascifolium and Tylophora ovata. Karbala Int J Mod Sci 1:237–246. https://doi.org/10.1016/j.kijoms.2015.12.003

Karthikeyan R, Mahalakshmi NV (2007) Performance and emission characteristics of a turpentine – diesel dual fuel engine. Energy 32:1202–1209. https://doi.org/10.1016/j.energy.2006.07.021

Kasiraman G, Geo VE, Nagalingam B (2016) Assessment of cashew nut shell oil as an alternate fuel for CI (Compression ignition) engines. Energy 101:402–410. https://doi.org/10.1016/j.energy.2016.01.086

Kasiraman G, Nagalingam B, Balakrishnan M (2012) Performance , emission and combustion improvements in a direct injection diesel engine using cashew nut shell oil as fuel with camphor oil blending. Energy 47:116–124. https://doi.org/10.1016/j.energy.2012.09.022

Kshirsagar CM, Anand R (2017) Artificial neural network applied forecast on a parametric study of Calophyllum inophyllum methyl ester-diesel engine out responses. Appl Energy 189:555–567. https://doi.org/10.1016/j.apenergy.2016.12.045

Kumar AN, Raju KB, Kishore PS, Narayana K (2018) ScienceDirect Some experimental studies on effect of exhaust-gas recirculation on performance and emission characteristics of a compression- ignition engine fuelled with diesel and lemon-peel oil blends. Mater Today Proc 5:6138–6148. https://doi.org/10.1016/j.matpr.2017.12.220

Li L, Jianxin W, Zhi W, Jianhua X (2015) Combustion and emission characteristics of diesel engine fueled with diesel / biodiesel / pentanol fuel blends. Fuel 156:211–218. https://doi.org/10.1016/j.fuel.2015.04.048

Mahmudul HM, Hagos FY, Mamat R, Adam AA, Ishak WFW, Alenezi R (2017) Production, characterization and performance of biodiesel as an alternative fuel in diesel engines – a review. Renew Sust Energ Rev 72:497–509. https://doi.org/10.1016/j.rser.2017.01.001

Manigandan S, Gunasekar P, Devipriya J, Nithya S (2019a) Emission and injection characteristics of corn biodiesel blends in diesel engine. Fuel 235:723–735. https://doi.org/10.1016/j.fuel.2018.08.071

Manigandan S, Gunasekar P, Poorchilamban S et al (2019b) Experimental investigation of the e ff ect of orifices inclination angle in multihole diesel injector nozzles . Part 2 – Spray characteristics. Fuel:1. https://doi.org/10.1080/15567036.2019.1587048

Manigandan S, Gunasekar P, Poorchilamban S, Nithya S, Devipriya J, Vasanthkumar G (2019c) Effect of addition of hydrogen and TiO2 in gasoline engine in various exhaust gas recirculation ratio. Int J Hydrog Energy 23;44(21):11205–18.

Mostafa S, Pierantozzi M, Moghadasi J (2019) Viscosities of some fatty acid esters and biodiesel fuels from a rough hard sphere-chain model and artificial neural network. Fuel 235:1083–1091. https://doi.org/10.1016/j.fuel.2018.08.088

Naser A, Haque A, Remadevi R, Naebe M (2018) Lemongrass (Cymbopogon) : a review on its structure, properties, applications and recent developments. Cellulose 25:5455–5477. https://doi.org/10.1007/s10570-018-1965-2

Noor CWM, Noor MM, Mamat R (2018) Biodiesel as alternative fuel for marine diesel engine applications : a review. Renew Sust Energ Rev 94:127–142. https://doi.org/10.1016/j.rser.2018.05.031

Parthasarathy M, Isaac Joshua Ramesh Lalvani J, Dhinesh B, Annamalai K (2016) Effect of hydrogen on ethanol–biodiesel blend on performance and emission characteristics of a direct injection diesel engine. Ecotoxicol Environ Saf 134:433–439. https://doi.org/10.1016/j.ecoenv.2015.11.005

Petranović Z, Bešenić T, Vujanović M, Duić N (2017) Modelling pollutant emissions in diesel engines, influence of biofuel on pollutant formation. J Environ Manag 203:1038–1046. https://doi.org/10.1016/j.jenvman.2017.03.033

Purushothaman K, Nagarajan G (2009a) Performance, emission and combustion characteristics of a compression ignition engine operating on neat orange oil. Renew Energy 34:242–245. https://doi.org/10.1016/j.renene.2008.03.012

Purushothaman K, Nagarajan G (2009b) Experimental investigation on a C. I. engine using orange oil and orange oil with DEE. Fuel 88: 1732–1740. https://doi.org/10.1016/j.fuel.2009.03.032

Rahman SMA, Van TC, Hossain FM et al (2019) Fuel properties and emission characteristics of essential oil blends in a compression ignition engine. Fuel 238:440–453. https://doi.org/10.1016/j.fuel.2018.10.136

Ramalingam K, Kandasamy A, James P, et al (2019) Production of eco-friendly fuel with the help of steam distillation from new plant source and the investigation of its influence of fuel injection strategy in diesel engine

Ramalingam KM, Kandasamy A, Subramani L et al (2018) An assessment of combustion, performance characteristics and emission control strategy by adding anti-oxidant additive in emulsified fuel. Atmos Pollut Res:1. https://doi.org/10.1016/j.apr.2018.02.007

Rao KP, Babu TV, Anuradha G et al (2017) IDI diesel engine performance and exhaust emission analysis using biodiesel with an artificial neural network (ANN). Egypt J Pet 26:593–600. https://doi.org/10.1016/j.ejpe.2016.08.006

Roy S, Banerjee R, Das AK, Bose PK (2014) Journal of Natural Gas Science and Engineering Development of an ANN based system identi fi cation tool to estimate the performance-emission characteristics of a CRDI assisted CNG dual fuel diesel engine. J Nat Gas Sci Eng 21:147–158. https://doi.org/10.1016/j.jngse.2014.08.002

Sakthivel R, Ramesh K, Purnachandran R, Shameer PM (2018) A review on the properties, performance and emission aspects of the third generation biodiesels. Renew Sust Energ Rev 82:2970–2992. https://doi.org/10.1016/j.rser.2017.10.037

Sarıtas I, Emre H, Og H (2010) Expert systems with applications prediction of diesel engine performance using biofuels with artificial neural network. Expert Systems with Applications 37:6579–6586. https://doi.org/10.1016/j.eswa.2010.02.128

Sathiyamoorthi R, Sankaranarayanan G (2016) Effect of antioxidant additives on the performance and emission characteristics of a DICI engine using neat lemongrass oil – diesel blend. FUEL 174:89–96. https://doi.org/10.1016/j.fuel.2016.01.076

Sathiyamoorthi R, Sankaranarayanan G (2017) The effects of using ethanol as additive on the combustion and emissions of a direct injection diesel engine fuelled with neat lemongrass oil-diesel fuel blend. Renew Energy 101:747–756. https://doi.org/10.1016/j.renene.2016.09.044

Selvan SS, Pandian PS, Saravanan ASS (2018a) Comparison of response surface methodology (RSM) and artificial neural network (ANN) in optimization of Aegle marmelos oil extraction for biodiesel production. Arab J Sci Eng 43:6119–6131. https://doi.org/10.1007/s13369-018-3272-5

Selvan SS, Pandian PS, Subathira A, Saravanan S (2018b) Saraca asoca seeds – a novel candidature for biodiesel production : studies on yield optimization using ANN coupled GA and properties of biodiesel blends. Int J Green Energy 00:1–12. https://doi.org/10.1080/15435075.2018.1529586

Srithar K (2017) Experimental investigations on mixing of two biodiesels blended with diesel as alternative fuel for diesel engines. J King Saud Univ - Eng Sci 29:50–56. https://doi.org/10.1016/j.jksues.2014.04.008

Subramani L, Parthasarathy M, Balasubramanian D (2018) Novel Garcinia gummi-gutta methyl ester (GGME) as a potential alternative feedstock for existing unmodified DI diesel engine. Renew Energy 125:568–577. https://doi.org/10.1016/j.renene.2018.02.134

Suresh M, Jawahar CP, Richard A (2018) A review on biodiesel production , combustion , performance , and emission characteristics of non-edible oils in variable compression ratio diesel engine using biodiesel and its blends. Renew Sust Energ Rev 92:38–49. https://doi.org/10.1016/j.rser.2018.04.048

Szabados G, Bereczky Á, Ajtai T, Bozóki Z (2018) Evaluation analysis of particulate relevant emission of a diesel engine running on fossil diesel and different biofuels. Energy 161:1139–53

Tamilselvan P, Nallusamy N, Rajkumar S (2017) A comprehensive review on performance, combustion and emission characteristics of biodiesel fuelled diesel engines. Renew Sust Energ Rev 79:1134–1159. https://doi.org/10.1016/j.rser.2017.05.176

Tosun E, Aydin K, Bilgili M (2016) Comparison of linear regression and artificial neural network model of a diesel engine fueled with biodiesel-alcohol mixtures. Alex Eng J 55:3081–3089. https://doi.org/10.1016/j.aej.2016.08.011

Uyumaz A (2018) Combustion , performance and emission characteristics of a DI diesel engine fueled with mustard oil biodiesel fuel blends at different engine loads. Fuel 212:256–267. https://doi.org/10.1016/j.fuel.2017.09.005

Vallinayagam R, Vedharaj S, Yang WM, Roberts WL, Dibble RW (2015) Feasibility of using less viscous and lower cetane (LVLC) fuels in a diesel engine: a review. Renew Sust Energ Rev 51:1166–1190. https://doi.org/10.1016/j.rser.2015.07.042

Vallinayagam R, Vedharaj S, Yang WM, Saravanan CG, Lee PS, Chua KJE, Chou SK (2014a) Impact of pine oil biofuel fumigation on gaseous emissions from a diesel engine. Fuel Process Technol 124:44–53. https://doi.org/10.1016/j.fuproc.2014.02.012

Vallinayagam R, Vedharaj S, Yang WM, Saravanan CG, Lee PS, Chua KJE, Chou SK (2014b) Impact of ignition promoting additives on the characteristics of a diesel engine powered by pine oil – diesel blend. Fuel 117:278–285. https://doi.org/10.1016/j.fuel.2013.09.076

Vallinayagam R, Vedharaj S, Yang WM, Lee PS, Chua KJE, Chou SK (2013) Combustion performance and emission characteristics study of pine oil in a diesel engine. Energy 57:344–351. https://doi.org/10.1016/j.energy.2013.05.061

Vallinayagam R, Vedharaj S, Yang WM, Lee PS, Chua KJE, Chou SK (2014c) Pine oil – biodiesel blends : a double biofuel strategy to completely eliminate the use of diesel in a diesel engine. Appl Energy 130:466–473. https://doi.org/10.1016/j.apenergy.2013.11.025

Verma P, Sharma MP (2016) Review of process parameters for biodiesel production from different feedstocks. Renew Sust Energ Rev 62: 1063–1071. https://doi.org/10.1016/j.rser.2016.04.054

Vigneswaran R, Annamalai K, Dhinesh B, Krishnamoorthy R (2018) Experimental investigation of unmodified diesel engine performance, combustion and emission with multipurpose additive along with water-in- diesel emulsion fuel. Energy Convers Manag 172: 370–380. https://doi.org/10.1016/j.enconman.2018.07.039

Wang Y, Gao W (2018) Environmental Effects Prediction of the water content of biodiesel using ANN-MLP : an environmental application. Energy Sources Part A Recover Util Environ Eff 40:987–993. https://doi.org/10.1080/15567036.2018.1468510